Upregulated RIP3 Expression Potentiates MLKL Phosphorylation–Mediated Programmed Necrosis in Toxic Epidermal Necrolysis

Sue Kyung Kim[1,6], Woo-Jung Kim[2,3,6], Jung-Ho Yoon[2,3], Jae-Hoon Ji[4], Michael J. Morgan[5], Hyeseong Cho[2,3], You Chan Kim[1] and You-Sun Kim[2,3]

Toxic epidermal necrolysis (TEN) is a severe adverse drug reaction involving extensive keratinocyte death in the epidermis. Histologically, the skin from TEN patients exhibits separation at the dermo–epidermal junction and accompanying necrosis of epidermal keratinocytes. Receptor-interacting protein kinase-3 (RIP3 or RIPK3) is an essential part of the cellular machinery that executes "programmed", or "regulated", necrosis and has a key role in spontaneous cell death and inflammation in keratinocytes under certain conditions. Here we show that RIP3 expression is highly upregulated in skin sections from TEN patients and may therefore contribute to the pathological damage in TEN through activation of programmed necrotic cell death. The expression level of mixed lineage kinase domain-like protein (MLKL), a key downstream component of RIP3, was not significantly different in skin lesions of TEN. However, elevated MLKL phosphorylation was observed in the skin from TEN patients, indicating the presence of RIP3-dependent programmed necrosis. Importantly, in an *in vitro* model of TEN, dabrafenib, an inhibitor of RIP3, prevented RIP3-mediated MLKL phosphorylation and decreased cell death. Results from this study suggest that the high expression of RIP3 in keratinocytes from TEN patients potentiates MLKL phosphorylation/activation and necrotic cell death. Thus, RIP3 represents a potential target for treatment of TEN.

Journal of Investigative Dermatology (2015) **135,** 2021–2030; doi:10.1038/jid.2015.90; published online 2 April 2015

INTRODUCTION

Toxic epidermal necrolysis (TEN) is a blistering disease most commonly caused by inappropriate immune activation in response to drugs. TEN is characterized by marked epidermal keratinocyte cell death with separation at the dermo–epidermal junction and lesions that show evidence of necrosis (Pereira *et al.*, 2007). Although rare, it has a mortality rate of 30% (Ghislain and Roujeau, 2002). TEN occurs in all ages but is more commonly seen in the immunosuppressed (Downey *et al.*, 2012). The pathophysiology is not well known, although immune mechanisms and altered drug metabolism are potentially responsible (Downey *et al.*, 2012). An association between the antiepileptic drug carbamazepine and major histocompatibility complex I allotype HLA-B*1502 exists in some races with TEN, (Man *et al.*, 2007; Mehta *et al.*, 2009; Chang *et al.*, 2011; Wei *et al.*, 2012), but not in others (Kaniwa *et al.*, 2008; Kim *et al.*, 2011), suggesting that genetic factors may predispose to TEN.

Little is known about the precise molecular events leading to the epidermal necrolysis observed in TEN, but FasL-mediated cell death and reactive oxygen species (ROS) have been implicated (Abe, 2008; Murata *et al.*, 2008). Epidermal tumor necrosis factor-α (TNF-α) found in TEN patients may contribute to ROS generation through stimulation of nitric oxide production (Kroncke *et al.*, 1997). Other reports suggest that keratinocyte death in TEN lesions is induced by granulysin exocytosed from CD8 T cells or natural killer cells (Chung *et al.*, 2008). When cellular FLICE-inhibitory protein expression is abrogated in the skin, severe cutaneous inflammation with cell death develops (Panayotova-Dimitrova *et al.*, 2013), suggesting that cellular FLICE-inhibitory protein levels may be relevant in TEN.

Programmed necrosis is activated in response to death receptor ligands and other cellular stressors (Declercq *et al.*, 2009; Vandenabeele *et al.*, 2010; Vanlangenakker *et al.*, 2012b). Programmed or "regulated" necrotic cell death is different

[1]*Department of Dermatology, Ajou University School of Medicine, Suwon, Korea;* [2]*Department of Biochemistry, Ajou University School of Medicine, Suwon, Korea;* [3]*Department of Biomedical Sciences, Graduate School, Ajou University, Suwon, Korea;* [4]*Genomic Instability Research Center, Ajou University School of Medicine, Suwon, Korea and* [5]*Department of Pharmacology, University of Colorado School of Medicine, Aurora, Colorado, USA*

Correspondence: You-Sun Kim, Department of Biochemistry, Ajou University School of Medicine, San 5, Wonchon-dong, Yeongtong-gu, Suwon 443-749, Korea. E-mail: yousunkim@ajou.ac.kr

[6]*These authors contributed equally to this work.*

Abbreviations: MLKL, mixed lineage kinase domain-like protein; RIP3 or RIPK3, receptor-interacting protein kinase-3; ROS, reactive oxygen species; SNP, sodium nitroprusside; TCZ, TNF-α+cycloheximide+zVAD; TEN, toxic epidermal necrolysis; TSZ, TNF-α+SMAC mimetic+zVAD

Received 19 September 2014; revised 7 February 2015; accepted 11 February 2015; accepted article preview online 6 March 2015; published online 2 April 2015

from apoptosis in that caspases are not essential for cell death to occur, but necrotic events lead to membrane permeability and cell lysis (Galluzzi *et al.*, 2012). Inhibition of this pathway is essential for proper mammalian development (Kaiser *et al.*, 2011; Oberst *et al.*, 2011; Zhang *et al.*, 2011) and prevents spontaneous cell death and inflammation in keratinocytes (Kovalenko *et al.*, 2009; Bonnet *et al.*, 2011). (The use of the terms "programmed necrotic cell death" or "programmed necrosis" are used herein in a wider context than development, designating all death that occurs using the specific necrotic cell machinery for this kind of death. Others use these terms in a more restrictive manner, designating only normal developmental cell death).

The programmed necrotic pathway includes the formation of a "necrosome" or a "Ripoptosome" complex containing receptor-interacting protein kinases RIP3(RIPK3) and RIP1 (RIPK1) and recruitment of mixed lineage kinase domain-like protein (MLKL; Sun *et al.*, 2012; Zhao *et al.*, 2012). The Ripoptosome complex is relevant to cell death pathways in keratinocytes, and its activity is regulated by cIAP proteins and cellular FLICE-inhibitory protein isoforms (Feoktistova *et al.*, 2011). RIP3-dependent phosphorylation and plasma membrane localization of MLKL is necessary for programmed necrotic cell death and leads to membrane permeabilization and cell death (Cai *et al.*, 2014; Chen *et al.*, 2014). Marion *et al.* reported sensitization of keratinocytes to RIP3-mediated necrosis as a potent mechanism triggering skin inflammation and proposed that factors sensitizing keratinocytes to programmed necrosis could contribute to inflammatory skin diseases and chronic inflammation (Bonnet *et al.*, 2013). Several reports suggest that high expression of RIP3 functions in inflammatory disease pathogenesis (Wu *et al.*, 2012; Pierdomenico *et al.*, 2014).

Here we show that RIP3 protein expression is highly elevated in TEN and may therefore contribute to cytotoxicity in TEN keratinocytes through potentiation of programmed necrotic cell death. We found elevated levels of phosphorylated MLKL in TEN lesions, suggesting that programmed necrosis is active. As RIP3 expression regulates the sensitivity of keratinocytes to necrotic stimuli, we propose that high RIP3 expression may contribute to TEN pathology and RIP3 could represent potential drug target for the management of TEN in patients.

RESULTS

RIP3 expression is substantially increased in TEN lesions

We analyzed RIP3 protein expression in the skin tissue from TEN patients with marked epidermal keratinocyte cell death. The TEN patients exhibited multiple erythematous macules evolving to bullae and epidermal detachment on the trunk (Figure 1a). Figure 1b shows clinical characteristics and laboratory results from our TEN patients ($n=10$), including age, heart rate, affected body surface area, and serum glucose levels, all of which are important prognostic factors for TEN patients. C-reactive protein levels, which rapidly rise in response to inflammation, were positively correlated with RIP3 expression in the lesional skin of TEN patients, as measured by immunohistochemistry (Figure 1b, right). This makes sense given that programmed necrosis can trigger inflammation (Kaczmarek *et al.*, 2013). Normal skin exhibited intact epidermis, but lesional skin from TEN showed eosinophilic necrosis of the epidermis, with some detachment from the dermis (Figure 1c and d). Comparable immunohistochemistry sections showed a significant increase in RIP3 expression levels when compared with normal skin. Quantification using an image analysis program indicated that RIP3 expression in the epidermal area (pigmented area per measured epidermal area) was significantly increased in the TEN skin compared with normal skin (Figure 1c and d).

In contrast to RIP3, expression of the downstream effector MLKL was not statistically different in TEN skin compared with normal skin (Figure 1e). Antibody specificity of the RIP3 and MLKL antibodies was confirmed by overexpression or knockdown of these two proteins, respectively, in several types of cells (Supplementary Figures S1A–C, S2A online). In addition, antibodies against GP100, which is commonly used to detect epidermal melanocytes, and Ki-67, which normally is an indicator of cell proliferation, stained similarly in normal skin and TEN lesions (Supplementary Figure S2B online), indicating that the detected RIP3 differences were not due to general issues with staining of the TEN lesion samples.

Canonical programmed necrosis can be executed in skin cells

As high expression of RIP3 could have a role in necrolysis in TEN patients, we first investigated whether skin cells were capable of executing programmed necrosis. All skin cell types examined, including primary melanocytes, fibroblasts, and keratinocytes, expressed RIP3 (Supplementary Figure S3A online). The immortal human keratinocyte line HaCaT and primary human epidermal keratinocyte (HEKn) isolated from neonatal foreskin responded to prototypical programmed necrotic stimuli (Supplementary Figure S3B online) induced by TNF-α (TNF-α+zVAD+either cycloheximide or SMAC mimetic, also referred to herein as TCZ or TSZ). Inhibition of caspase activity by zVAD completely blocked caspase-3 and PARP processing (data not shown), but did not prevent TNF-induced cell death, indicating that RIP3-expressing keratinocytes are capable of dying by prototypical programmed necrosis, similar to what is observed in the human colon adenocarcinoma HT-29 cell line (Supplementary Figure S3C online), which is a standard model for the study of programmed necrosis. As expected, RIP3 (and RIP1) knockout mouse embryonic fibroblasts were resistant to TNF-induced necrotic cell death conditions (Supplementary Figure S4A online), consistent with the roles of these proteins in programmed necrosis. Similarly, knockdown of RIP3 effectively reduced TNF-induced necrotic cell death in human dermal fibroblast and HaCaT cells, indicating that RIP3 is essential for programmed necrosis in skin cells (Supplementary Figure S4B online). Thus, the canonical programmed necrotic pathway can be executed in skin cells.

SNP-induced keratinocyte cell death is accompanied by RIP3-dependent programmed necrosis

Lesional skin of TEN patients is characterized by high levels of inducible nitric oxide synthase and associated nitric oxide (NO) production and is believed to contribute to TEN

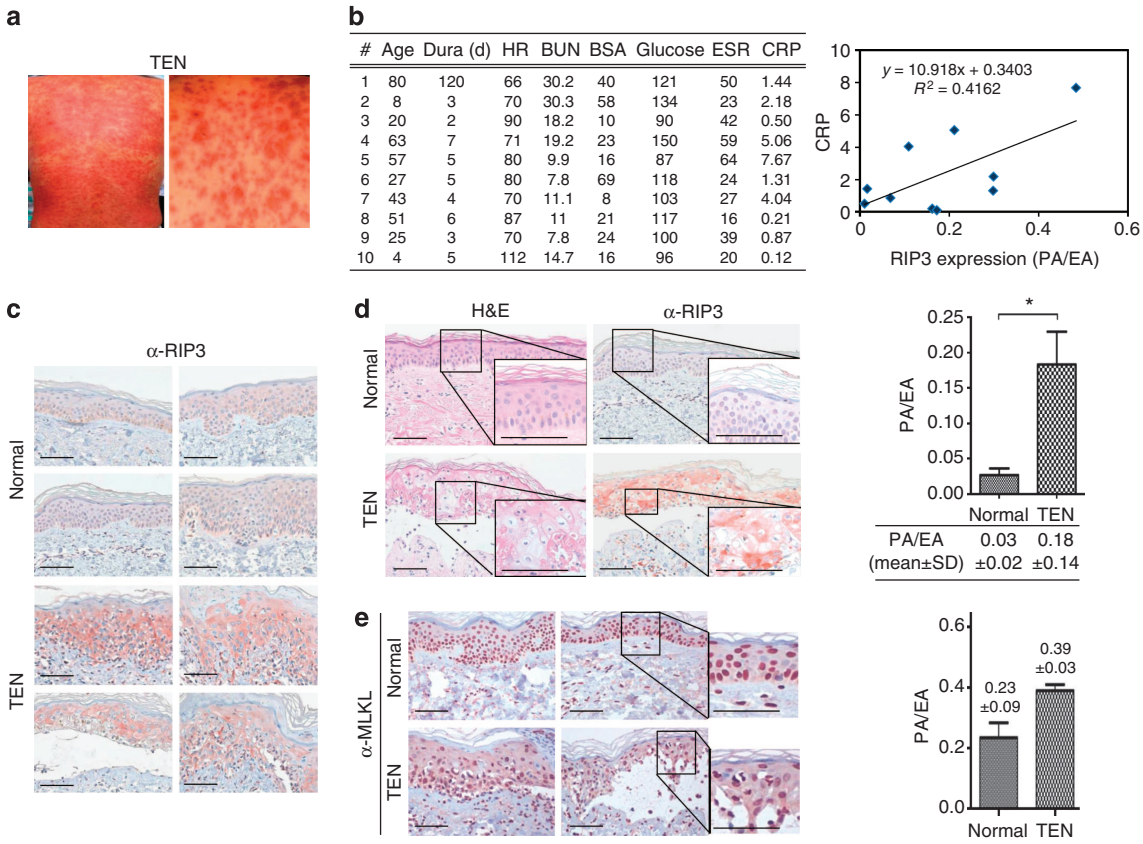

#	Age	Dura (d)	HR	BUN	BSA	Glucose	ESR	CRP
1	80	120	66	30.2	40	121	50	1.44
2	8	3	70	30.3	58	134	23	2.18
3	20	2	90	18.2	10	90	42	0.50
4	63	7	71	19.2	23	150	59	5.06
5	57	5	80	9.9	16	87	64	7.67
6	27	5	80	7.8	69	118	24	1.31
7	43	4	70	11.1	8	103	27	4.04
8	51	6	87	11	21	117	16	0.21
9	25	3	70	7.8	24	100	39	0.87
10	4	5	112	14.7	16	96	20	0.12

Figure 1. Upregulation of receptor-interacting protein kinase-3 (RIP-3) in TEN lesions. (**a**) Photograph of a TEN patient showing confluent and erythematous macules and patches with flaccid bullae and epidermal detachment. (**b**) Left: clinical characteristics and laboratory results for TEN patients ($n = 10$). Right: RIP3 expression in lesional skin is positively correlated with plasma CRP levels in TEN patients. (**c**-**d**) Left: immunohistochemical staining indicates that RIP3 expression is increased in TEN skin compared with normal skin. H&E staining shows lesional skin of TEN with eosinophilic epidermal necrosis and separation of dermo–epidermal junction, whereas normal skin is intact. Right: quantitative image analysis of RIP3 staining. (**e**) Immunohistochemical staining and quantitative image analysis showing that expression of MLKL in TEN lesional skin is not significantly different than normal skin (black scale bar = 100 μm). CRP, C-reactive protein; H&E, hematoxylin and eosin; MLKL, mixed lineage kinase domain-like protein; PA/EA, pigmented area per measured epidermal area; TEM, toxic epidermal necrolysis.

pathology (Schwartz *et al.*, 2013). Previous studies have employed sodium nitroprusside (SNP), an NO donor, as a model agent (Viard-Leveugle *et al.*, 2013). As SNP does not induce RIP3 expression (or TNF-α) (Supplementary Figure S5 online), this suggests that induction of RIP3 occurs upstream and independently of NO production in TEN and that SNP could be used to look at the downstream consequences of NO production in TEN after RIP3 has been highly expressed. SNP treatment of HaCaT and HEKn cells induced dose-dependent cell death (Figure 2a; Supplementary Figure S6A online) and phosphorylation of mitogen-activated protein kinase (Figure 2b). The pancaspase inhibitor zVAD had only a small effect on SNP-induced cell death, although it completely blocked caspase-3 and PARP processing induced by TNF/CHX and SNP (Supplementary Figure S6B online). SNP-induced cell death was more substantially decreased in the presence of necrostatin-1 (Nec-1), an inhibitor of RIPK1 and programmed necrosis (Degterev *et al.*, 2008); the further combination of zVAD and Nec-1 had a more pronounced inhibitory effect upon SNP-induced cell death (Figure 2c, top), suggesting that SNP activates both apoptosis and programmed necrosis. Phase-contrast microscopy and annexin-V staining as monitored by flow cytometry in HaCaT cells likewise indicated that SNP-induced cell death was inhibited by these compounds, with Nec-1 being more potent (Figure 2c, bottom). We therefore also tested other pharmacological inhibitors of programmed necrosis–dabrafenib, which inhibits RIP3 kinase activity (Li *et al.*, 2014a), and necrosulfonamide, which inhibits MLKL functions downstream of RIP3 phosphorylation (Wang *et al.*, 2014). All three inhibitors were substantially better at protecting HEKn cells from the acute SNP cytotoxicity than zVAD, which had little effect (Figure 2d; Supplementary Figure S6C online).

RIP3 and RIP1 potentiate SNP-induced keratinocyte cell death

RIP3 knockout mouse embryonic fibroblasts ectopically expressing RIP3 became more sensitive to SNP-mediated cell death (Supplementary Figure S7A online), whereas knock-down of RIP3 in HaCaT, primary keratinocytes (HEKn), or human dermal fibroblasts inhibited SNP-induced cell death

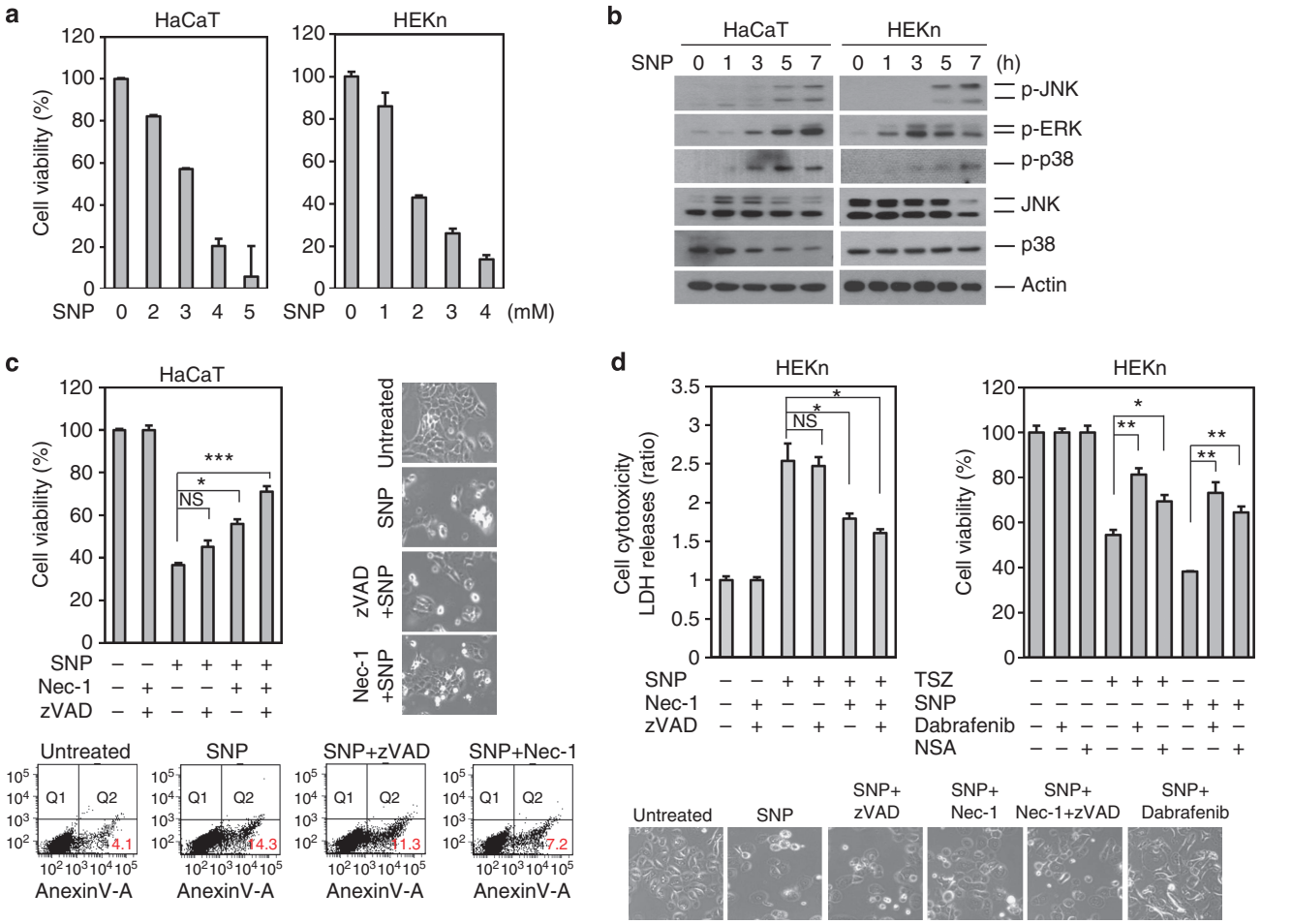

Figure 2. Programmed necrosis inhibitors reduce sodium nitroprusside (SNP)-induced keratinocyte cell death. (**a**) The MTT assay showing viability of HaCaT and HEKn cells treated with indicated concentrations of SNP (24 hours). (**b**) Western blots showing mitogen-activated protein kinase activation in HaCaT and HEKn cells in response to SNP (5 mM) for indicated time points. (**c**) The MTT assay (left panel) and phase-contrast microscopy (right panel) showing cells pretreated with Nec-1 (80 μM) or/and zVAD (20 μM) for 1 hour followed by SNP treatment. Bottom panel shows annexin-V staining measured by FACS analysis. (**d**) Cells were pretreated with Nec-1 or/and zVAD (left panel) or dabrafenib (10 μM) or necrosulfonamide (NSA, 0.5 μM; right panel) for 1 hour followed by SNP or TSZ treatment (24 hours) and cell viability analyzed by LDH release (left panel). The MTT assay (right panel) or phase-contrast microscopy (bottom panel). All results are averages ± SEM. $^{*}P<0.05$, $^{**}P<0.01$, and $^{***}P<0.005$. HEKn, human epidermal keratinocyte; LDH, lactate dehydrogenase.

(Supplementary Figure S7B online; Figure 3a and b). Consistent with Nec-1 inhibition, RIP-1 knockdown inhibited SNP-induced cell death in the HaCaT cells (Supplementary Figure S7C online), further suggesting that RIP1/RIP3-dependent programmed necrosis contributes to SNP-induced cell death.

Sustained activation of the stress kinases c-Jun N-terminal kinase (JNK) and p38 is often associated with programmed necrosis and is essential for cell death in some cell types (Ventura *et al.*, 2004; Kim *et al.*, 2007). Sustained SNP-induced JNK and p38 activation, but not ERK (extracellular signal–regulated kinase) activation, was inhibited in RIP3 knockdown cells (Figure 3c); however, under non-necrotic conditions (i.e., no zVAD/CHX), TNF-induced JNK and p38 activation remained relatively normal in the absence of RIP3 (Supplementary Figure S7D online), consistent with their sustained activation downstream of RIP3 during programmed necrosis.

In order to examine the functional consequence of high RIP3 expression in TEN, we ectopically expressed RIP3 in HaCaT and HEKn cells (Figure 4a). Cells overexpressing RIP3 were more sensitive to SNP, especially after 6 hours (Figure 4b), indicating that high expression of RIP3 is sufficient to promote SNP sensitivity. Thus, high expression of RIP3 in TEN may potentiate the pathological process by sensitizing to necrotic stimuli.

We (and others) have previously shown that, in some cases, the induction of ROS and sustained JNK activation can contribute to necrotic cell death (Kim *et al.*, 2007; Wu *et al.*, 2011). In the RIP3-overexpressing cells, TNF-induced JNK activation remained relatively normal under non-necrotic conditions (i.e., no zVAD/CHX), but sustained activation of JNK was potentiated upon a necrotic stimulus (TCZ; Supplementary Figure S8A and B online). Likewise, activation of JNK and p38 by SNP was potentiated in RIP3-expressing

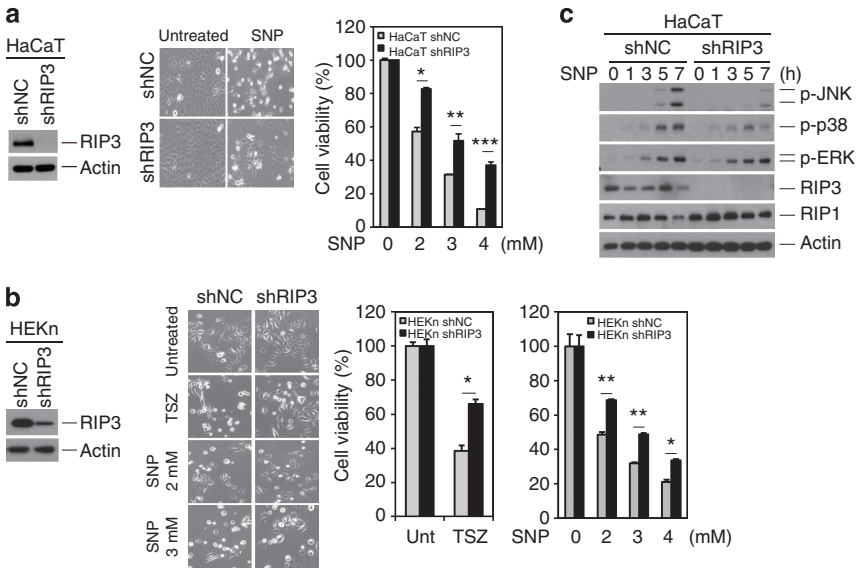

Figure 3. Depletion of receptor-interacting protein kinase-3 (RIP-3) inhibits sodium nitroprusside (SNP)-induced keratinocyte cell death. (**a**) HaCaT cells with stable shRIP3 integration (left panel) were treated with SNP for 24 hours, and cell viability was analyzed by phase-contrast microscopy (middle panel) and the MTT assay (right panel). (**b**) HEKn cells with stable shRIP3 integration (left panel) were treated with SNP or TSZ for 24 hours, and cell viability was analyzed by phase-contrast microscopy (middle panel) and the MTT assay (right panel). (**c**) Western blotting showing lysates from cells treated with SNP for indicated time points, indicating that RIP3 knockdown reduces p-JNK and p-p38 but not p-ERK. All results shown are averages ± SEM. $*P<0.05$, $**P<0.01$, and $***P<0.005$. ERK, extracellular signal–regulated kinase; HEKn, human epidermal keratinocyte.

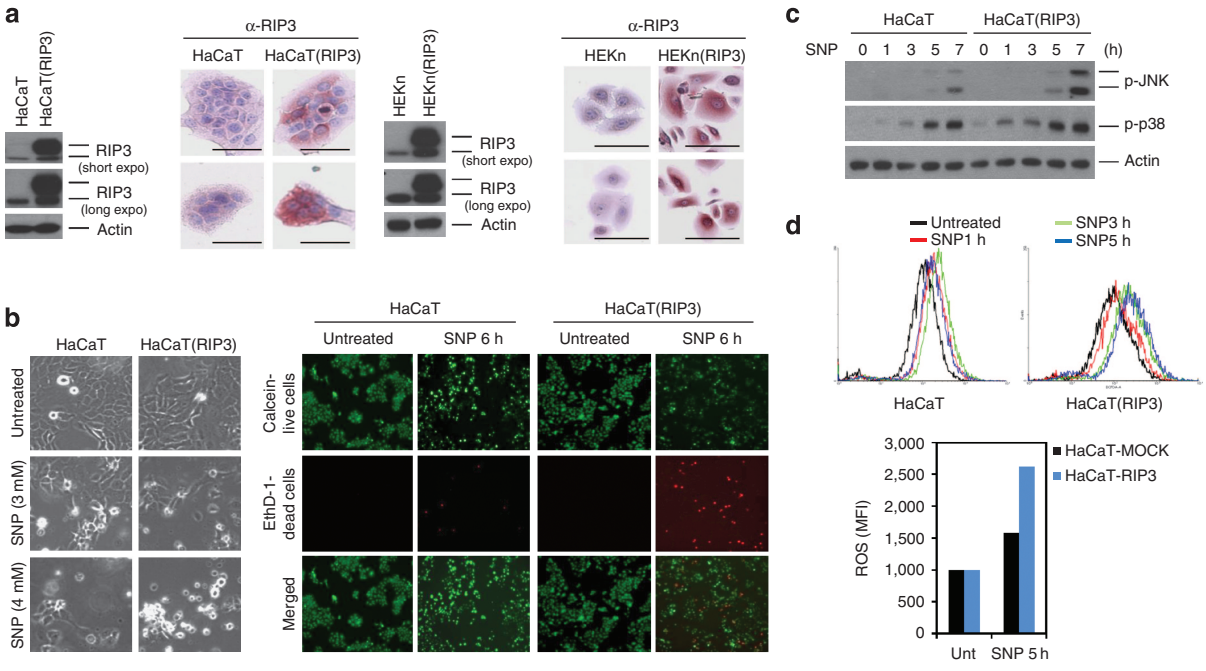

Figure 4. High expression of receptor-interacting protein kinase-3 (RIP-3) leads to increased reactive oxygen species (ROS) production and potentiated mitogen-activated protein kinase activation. (**a**) HaCaT and HEKn cells were infected with pLX303-hRIP3 lentiviral plasmid to establish stable RIP3-overexpressing cells. RIP3 expression was confirmed by western blot (left panel) and immunohistochemistry (right panel; black scale bar = 50 μm). (**b**) Left panel: cells from **a** were treated with different concentrations with SNP (18 hours), and cell viability was analyzed by microscopy. Right panel: cells treated with SNP (5 mM, 6 hours) were analyzed by the calcein/EthD-1 live/dead assay (right panel). (**c**) Western blotting of cells treated with SNP (5 mM) for indicated time points. (**d**) Cells were treated with SNP (5 mM) for indicated time points, and ROS generation (DCFH-DA) was measured by FACS or was visualized by fluorescence microscopy (right panel). HEKn, human epidermal keratinocyte; SNP, sodium nitroprusside.

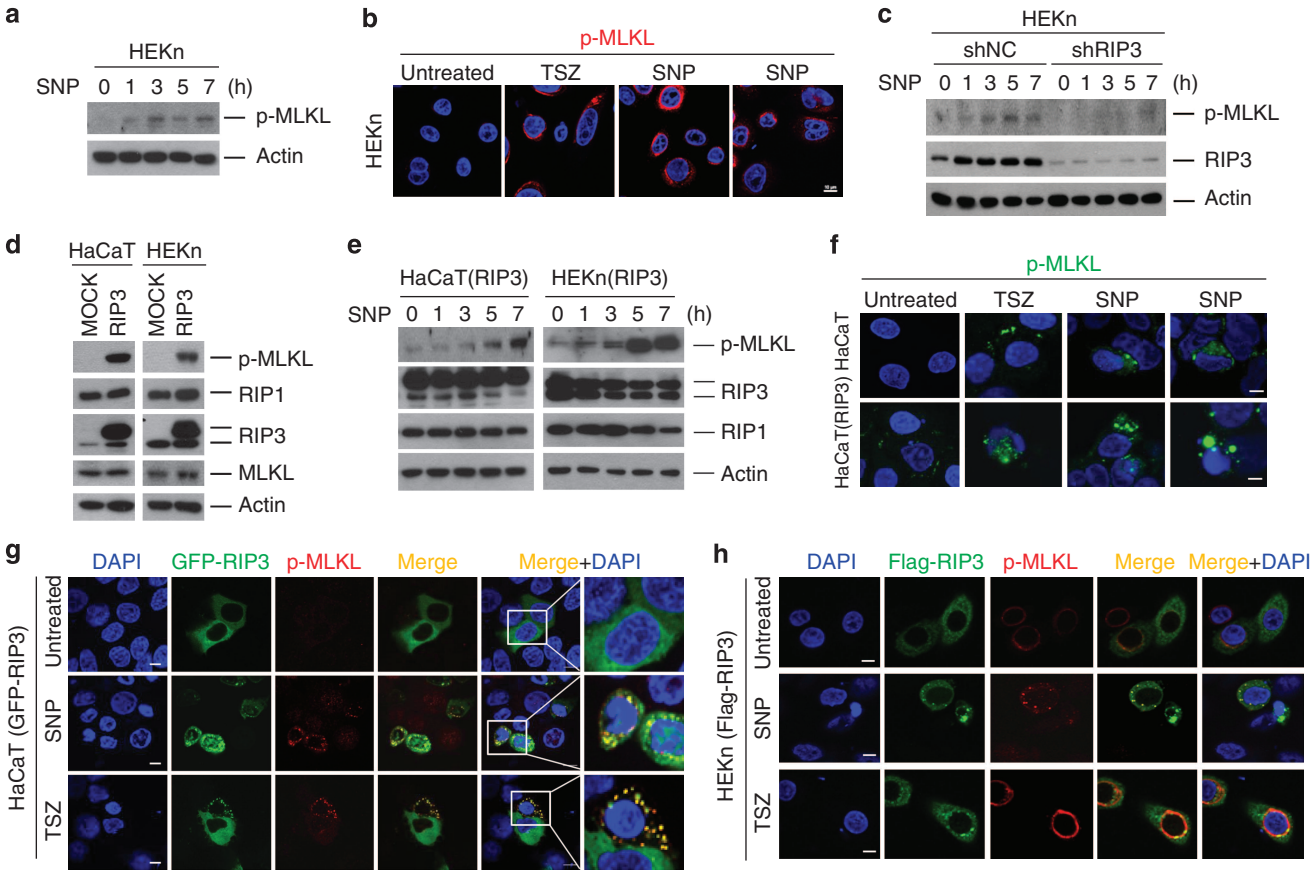

Figure 5. Sodium nitroprusside (SNP) induces mixed lineage kinase domain-like protein (MLKL) phosphorylation downstream of receptor-interacting protein kinase-3 (RIP-3) activation. (**a**) Western blots of lysates from HEKn cells treated with SNP (5 mM) at indicated time points. (**b**) Confocal immunofluorescence pictures of phospho-MLKL in HEKn cells treated with TSZ or SNP (5 mM) for 6 hours. (**c**) Western blots of lysates from shRIP3-HEKn cells treated with SNP (5 mM). (**d** and **e**) Western blots of lysates from parental and RIP3-overexpressing HaCaT/HEKn cells. In **e**, cells were treated with SNP (5 mM), as indicated. (**f**) Immunostaining of phospho-MLKL in parental and RIP3-overexpressing HaCaT cells treated 6 hours with TSZ or SNP (3 mM). (**g**) HaCaT cells transfected with GFP-RIP3 plasmid and treated 6 hours with TSZ or SNP (5 mM) and immunostained for phospho-MLKL. (**h**) RIP3-overexpressing HEKn cells treated with TSZ or SNP (3 mM) for 6 hours and co-stained with phospho-MLKL(1:250) and Flag antibodies. White scale bar is 10 μm. HEKn, human epidermal keratinocyte.

cells (Figure 4c). As ROS inactivate JNK phosphatases, leading to JNK activity (Kamata *et al.*, 2005), we measured ROS production in response to SNP. ROS production was markedly increased in RIP3-overexpressing HaCaT cells (Figure 4d), suggesting that high RIP3 expression contributes to ROS generation and potentiates JNK activation during SNP-induced cell death. Importantly, pretreatment of the cells with the ROS scavenger N-acetylcysteine inhibited SNP-induced cell death to a similar extent as Nec-1 (Supplementary Figure S9A online), indicating that ROS contributes to SNP-induced cell death. SNP-induced cell death was inhibited by JNK, p38, and ERK inhibitors (Supplementary Figure S9B online). Thus, increased RIP3 may lead to increased ROS production, which may then activate JNK and p38 activation, further potentiating cell death.

High RIP3 expression contributes to cell death through MLKL activation

RIP3-dependent phosphorylation and subsequent plasma membrane localization of MLKL is necessary for programmed necrotic cell death (Cai *et al.*, 2014; Chen *et al.*, 2014). Phosphorylated MLKL was detected in HEKn cells treated with SNP (Figure 5a). Moreover, SNP-induced p-MLKL localized at the plasma membrane, similar to TSZ (Figure 5b). However, knockdown of RIP3 eliminated MLKL phosphorylation (Figure 5c), indicating that it was RIP3 dependent. In HaCaT and HEKn cells highly expressing RIP3, p-MLKL was observed in the absence of stimulus (Figure 5d). However, p-MLKL was further potentiated by SNP (Figure 5e) or TSZ (Supplementary Figure S10 online). In early-stage cells treated with SNP, p-MLKL was shown in punctate structures, similar to cells treated with TSZ (Figure 5f), before its translocation to the cell membrane. In RIP3-overexpressing HaCaT and HEKn cells treated with SNP, p-MLKL largely co-localized with RIP3 (Figure 5g and h) in these early-stage punctate bodies, similar to the pattern seen with TSZ treatment.

The basal phosphorylation of MLKL in RIP3-overexpressing cells, as well as SNP-induced p-MLKL, was eliminated by RIP3 inhibition with dabrafenib (Figure 6a, top), which

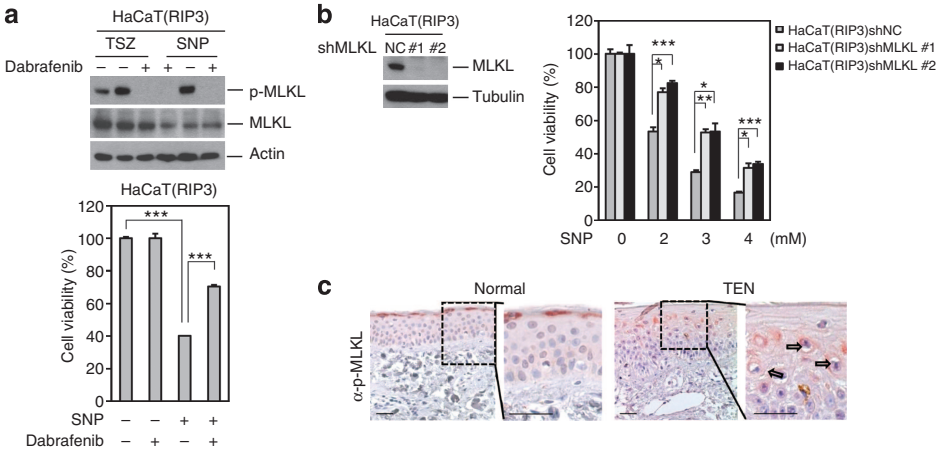

Figure 6. Receptor-interacting protein kinase-3 (RIP-3)-mediated mixed lineage kinase domainlike protein (MLKL) activation contributes to keratinocyte cell death. (**a**) Top panel: HaCaT cells were pretreated with dabrafenib (10 μM) for 1 hour and then treated with TSZ or SNP for 7 hours, and cell lysates were analyzed by western blot. Bottom panel: other cells were further treated for 24 hours and viability analyzed by the MTT assay. Results are averages ± SEM. (**b**) RIP3-expressing HaCaT cells were infected with a lentivirus-encoding MLKL shRNAs or non-silencing control. After selection with puromycin, cells with stable shRNA integration were analyzed by western blotting (left panel) or treated with SNP for 24 hours and viability analyzed by the MTT assay (right panel). Results are averages ± SEM. (**c**) Immunohistochemical staining of phospho-MLKL (1:100) in paraffin-embedded tissue specimens from TEN patients (black scale bar = 50 μm). $^{*}P<0.05$, $^{**}P<0.01$, and $^{***}P<0.005$. SNP, sodium nitroprusside; TEN, toxic epidermal necrolysis.

correlated with its effects on cell death (Figure 6a, bottom). Consistent with its mechanism of inhibition during necrosis downstream of phosphorylation, MLKL phosphorylation induced by SNP was not inhibited by necrosulfonamide (Data not shown), although it inhibited SNP-mediated cell death. Significantly, knockdown of MLKL in RIP3-HaCaT reduced cell death by SNP (Figure 6b), indicating that MLKL activation contributed to SNP-mediated cell death. Finally, and most importantly, elevated phosphorylation of MLKL was detected in the skin from TEN patients (Figure 6c), establishing its activation during TEN.

DISCUSSION

Programmed necrosis has been identified as an important mechanism underlying multiple physiological and pathological processes (Vanlangenakker *et al.*, 2012a; Kaczmarek *et al.*, 2013). We found that the RIP3 protein, a key regulator of programmed necrosis, was significantly increased in TEN skin compared with normal skin. In addition, we found elevated levels of phosphorylated MLKL in TEN samples, suggesting that programmed necrosis is activated and that the RIP3-MLKL pathway has an important role in TEN pathology.

Both TNF-α and inducible nitric oxide synthase, with accompanying NO production, have been implicated in the pathological process of TEN (Schwartz *et al.*, 2013). We found that skin cells, including keratinocytes, were sensitive to programmed necrosis in response to TNF-α and SNP, an NO donor. Previously, the NO donor SNP was reported to induce caspase-dependent apoptosis through upregulation of FasL (Schwartz *et al.*, 2013). In our hands, SNP-induced cell death was only partially blocked by treatment of the pan-caspase inhibitor zVAD but was significantly decreased by the programmed necrosis inhibitors Nec-1, NSA, and dabrafenib and decreased further by a combination of these inhibitors and zVAD. Furthermore, knockdown of RIP3 or MLKL resulted in inhibition of SNP-induced cell death. Thus, our data indicate that SNP not only initiates caspase activation but also induces programmed necrosis. Therefore, it is likely that programmed necrosis mediated by TNF-α and NO, which are found in abundance in TEN, is highly potentiated by the high RIP3 levels that are also found in TEN, resulting in greater cytotoxicity. As Fas ligand has been implicated in TEN (Abe, 2008; Murata *et al.*, 2008), it is also likely that high RIP3 levels may sensitize to this ligand, especially as a role for RIP1 in caspase-independent CD95 signaling in keratinocytes has been shown (Geserick *et al.*, 2009).

Dabrafenib inhibits the kinase activity of RIP3 (Li *et al.*, 2014b), and we have shown here that it inhibits TNF-α and SNP-induced programmed necrosis in keratinocytes and other skin cells. If RIP3 is important in TEN, then dabrafenib, which inhibits and is already FDA approved (as selective BRAF inhibitor) for the treatment of metastatic melanoma, may potentially be an effective drug for the treatment of TEN.

Although we were preparing this manuscript for publication, a work by Saito *et al.* (2014), was published that also suggests that necroptosis may contribute to the pathogenesis of TEN and the Stevens Johnson syndrome (SJS) . They identified annexin A1 secreted by monocytes as an important mediator of keratinocyte death in TEN/SJS and claim that annexin A1 binds to formyl peptide receptor 1, the receptor for annexin A1, and activates the necroptosis pathway through the RIP1/RIP3 complex. Although not rigorously analyzed on this point, their data does seem in agreement that RIP3 is highly expressed in TEN compared with normal. Furthermore, their data show that control skin/keratinocytes do not respond to necrotic stimuli as well as SJS/TEN lesions/keratinocytes do, consistent with our data showing that high RIP3 expression in TEN keratinocytes potentiates cell death in

response to such stimuli. If the conclusions of this study are true, annexin A1 may be an important necrotic stimulus that is potentiated by high RIP3 expression in TEN.

In summary, on the basis of our data, we suggest that programmed necrosis mediated by RIP3-MLKL contributes to the pathological state of the skin in TEN. Therefore, RIP3 could be a potential therapeutic target for the treatment of TEN.

MATERIALS AND METHODS

Reagents

Recombinant TNF-α and zVAD were from R&D Systems (Minneapolis, MN). Anti-phopho-JNK(44682G), anti-phospho-ERK (9101S), anti-phospho-p38(4511), anti-ERK(4695), anti-p38(9212), anti-PARP-1(9542S), and anti-caspase 3(9662) antibodies were from Cell Signaling (Danvers, MA). Anti-JNK antibody was from Invitrogen (Carlsbad, CA). Anti-RIP3(72106) and phospho-MLKL(187091) antibodies were from Abcam (Cambridge, MA). Nec-1, LPS, and MLKL (M6697) antibodies were purchased from Sigma-Aldrich (St. Louis, MO). Anti-GP100(7006-1) antibody was from Monosan (Uden, the Netherlands). Anti-Ki-67(15580) antibody was from Abcam. Necrosulfonamide and cycloheximide were from Calbiochem (Danvers, MA). Dabrafenib was from Selleckchem (Houston, TX). SMAC mimetic (LCL-161) was from Adooq Bioscience (Irvine, CA).

Patients

After obtaining informed written consent, we investigated 10 patients with TEN, which was confirmed clinically and pathologically, the clinical data collected by review of medical record, retrospectively. This study was approved by the institutional review board (IRB number: MED-KSP-13-029).

Immunohistochemistry and image analysis

Punch skin biopsy specimens (3 mm) were taken from 10 TEN patients. Five normal tissues from patients who had performed skin biopsy for diagnosis of pigmentary disease were used as controls. Paraffin-embedded tissue sections of 3-μm thickness were processed for light microscopic examination. Immunohistochemistry was performed using standard techniques using primary antibodies to RIP3, MLKL, p-MLKL, GP-100, and Ki-67. Quantitative analysis of immunohistochemical stains was performed using Image Pro Plus, Version 4.5 (Media Cybertics, Silver Spring, MD) on a representative area of each specimen. The ratio of stained area to the measured epidermal area (pigmented area per measured epidermal area) was measured in TEN skin lesions and normal skin.

Cell culture

All cells were cultured at 37 °C in 5% CO_2. Primary human dermal fibroblasts were previously described (Palmetshofer *et al*, 1995). Fibroblasts and HaCaT cells were cultured in DMEM supplemented with 10% fetal bovine serum, 2 mM glutamine, 100 U ml^{-1} penicillin, and 100 μg ml^{-1} streptomycin. Primary normal human keratinocyte was cultured as previously described (Pincelli *et al.*, 1994). Skin specimens obtained from repeat Caesarean section deliveries and circumcisions were used for cultures and grown in Epilife medium (Gibco BRL, Gaithersburg, MD) with human keratinocyte growth supplement (Gibco). Cells at passage 3–10 were used for experiments. HEKn cells were from Gibco and maintained according to the manufacturer's instructions in Epilife medium with human keratinocyte growth supplement. Cells at passage 3–6 were used for experiments. HaCaT/HEKn cells stably expressing RIP3 were created from cells infected with pLX303-hRIP3 lentiviral plasmid.

Cell viability assay

Representative images were taken by a phase-contrast microscope. Cell viability was determined using tetrazolium dye colorimetric tests (the MTT assay) read at 570 nm. Cell viability was also assessed by double labeling of cells with 2 μM calcein-AM and 4 μM EthD-1. Calcein-positive live cells and EthD-1-positive dead cells were visualized using fluorescence microscopy (Axiovert 200M, Zeiss, Jena, Germany). Lactate dehydrogenase leakage was quantified using a cytotoxicity detection kit (Promega, Madison, WI), or a FITC-Annexin V Apoptosis Detection kit (BD Pharmingen, San Jose, CA), according to the manufacturer's protocols.

Western blot analysis

Cells were lysed in M2 buffer (20 mM Tris at pH 7, 0.5% NP-40, 250 mM NaCl, 3 mM EDTA, 3 mM EGTA, 2 mM DTT, 0.5 mM PMSF, 20 mM β-glycerol phosphate, 1 mM sodium vanadate, and 1 μg ml^{-1} leupeptin). Equal cell extracts were resolved by 12% SDS-PAGE and analyzed by western blot using enhanced chemiluminescence (Amersham, Piscataway, NJ).

Immunostaining

HaCaT, HeLa, and HEKn cells were incubated on chamber slides and fixed by cold acetone (10 seconds). Immunohistochemical staining was performed using the avidin–biotin–peroxidase complex. For immunofluorescence, anti-phospho-MLKL was incubated overnight at 4 °C(1:250), and FITC-conjugated secondary antibody (goat anti-rabbit IgM, 1:500 dilution, Molecular Probes, Eugene, OR) was incubated 1 hour at room temperature. Representative images were taken by confocal microscope.

Measurement of intracellular ROS

Cells were incubated with 10 μM H_2 DCFDA for 30 minutes before the end of treatments. Increases in fluorescence were measured by FACS and by examination under a confocal microscope (Carl Zeiss LSM710).

Lentiviral shRNA experiments

Short-hairpin RNA (shRNA) plasmids targeting hRIP3 mRNA (NM_006871), mRIP3 mRNA (NM_019955), hMLKL mRNA (NM_152649), hRIP1 (NM_003804.3), and non-targeting control (NM_027088) were from Sigma-Aldrich. Lentiviral plasmids were transfected into 293TN cells (System Biosciences, Mountain View, CA). Pseudoviral particles were collected 2 days after the transfection and infected into cells with polybrene (8 μg ml^{-1}). Infected cells were puromycin selected 2 days after infection.

Statistics

Independent experiments were performed at least in triplicate. Statistical significance was evaluated in paired analyses using the Mann–Whitney *U*-test (nonparametric), depending on the data distribution. Data values are expressed as mean ± SEM. Statistical significance was considered $P<0.05$.

CONFLICT OF INTEREST

The authors state no conflict of interest.

ACKNOWLEDGMENTS

This research was supported by the Basic Science Research Program through the National Research Foundation of Korea (NRF), funded by grant (No. 2011-0030043 and 2014R1A2A1A11052951) to Y-SK from the Ministry of Education, Science, and Technology.

SUPPLEMENTARY MATERIAL

Supplementary material is linked to the online version of the paper at http://www.nature.com/jid

REFERENCES

Abe R (2008) Toxic epidermal necrolysis and Stevens-Johnson syndrome: soluble Fas ligand involvement in the pathomechanisms of these diseases. *J Dermatol Sci* 52:151–9

Bonnet MC, Bagot M, Bensussan A (2013) Apoptotic and necroptotic cell death in cutaneous inflammation. *Eur J Dermatol*. e-pub ahead of print 7 April 2013

Bonnet MC, Preukschat D, Welz PS *et al.* (2011) The adaptor protein FADD protects epidermal keratinocytes from necroptosis in vivo and prevents skin inflammation. *Immunity* 35:572–82

Cai Z, Jitkaew S, Zhao J *et al.* (2014) Plasma membrane translocation of trimerized MLKL protein is required for TNF-induced necroptosis. *Nat Cell Biol* 16:55–65

Chang CC, Too CL, Murad S *et al.* (2011) Association of HLA-B*1502 allele with carbamazepine-induced toxic epidermal necrolysis and Stevens-Johnson syndrome in the multi-ethnic Malaysian population. *Int J Dermatol* 50: 221–4

Chen X, Li W, Ren J *et al.* (2014) Translocation of mixed lineage kinase domain-like protein to plasma membrane leads to necrotic cell death. *Cell Res* 24: 105–21

Chung WH, Hung SI, Yang JY *et al.* (2008) Granulysin is a key mediator for disseminated keratinocyte death in Stevens-Johnson syndrome and toxic epidermal necrolysis. *Nat Med* 14:1343–50

Declercq W, Vanden Berghe T, Vandenabeele P (2009) RIP Kinases at the Crossroads of Cell Death and Survival. *Cell* 138:229–32

Degterev A, Hitomi J, Germscheid M *et al.* (2008) Identification of RIP1 kinase as a specific cellular target of necrostatins. *Nat Chem Biol* 4: 313–21

Downey A, Jackson C, Harun N *et al.* (2012) Toxic epidermal necrolysis: review of pathogenesis and management. *J Am Acad Dermatol* 66: 995–1003

Feoktistova M, Geserick P, Kellert B *et al.* (2011) cIAPs block Ripoptosome formation, a RIP1/caspase-8 containing intracellular cell death complex differentially regulated by cFLIP isoforms. *Mol Cell* 43: 449–63

Galluzzi L, Vitale I, Abrams JM *et al.* (2012) Molecular definitions of cell death subroutines: recommendations of the Nomenclature Committee on Cell Death 2012. *Cell Death Differ* 19:107–20

Geserick P, Hupe M, Moulin M *et al.* (2009) Cellular IAPs inhibit a cryptic CD95-induced cell death by limiting RIP1 kinase recruitment. *J Cell Biol* 187:1037–54

Ghislain PD, Roujeau JC (2002) Treatment of severe drug reactions: Stevens-Johnson syndrome, toxic epidermal necrolysis and hypersensitivity syndrome. *Dermatol Online J* 8:5

Kaczmarek A, Vandenabeele P, Krysko DV (2013) Necroptosis: the release of damage-associated molecular patterns and its physiological relevance. *Immunity* 38:209–23

Kaiser WJ, Upton JW, Long AB *et al.* (2011) RIP3 mediates the embryonic lethality of caspase-8-deficient mice. *Nature* 471:368–72

Kamata H, Honda S, Maeda S *et al.* (2005) Reactive oxygen species promote TNFalpha-induced death and sustained JNK activation by inhibiting MAP kinase phosphatases. *Cell* 120:649–61

Kaniwa N, Saito Y, Aihara M *et al.* (2008) HLA-B locus in Japanese patients with anti-epileptics and allopurinol-related Stevens-Johnson syndrome and toxic epidermal necrolysis. *Pharmacogenomics* 9:1617–22

Kim SH, Lee KW, Song WJ *et al.* (2011) Carbamazepine-induced severe cutaneous adverse reactions and HLA genotypes in Koreans. *Epilepsy Res* 97:190–7

Kim YS, Morgan MJ, Choksi S *et al.* (2007) TNF-induced activation of the Nox1 NADPH oxidase and its role in the induction of necrotic cell death. *Mol Cell* 26:675–87

Kovalenko A, Kim JC, Kang TB *et al.* (2009) Caspase-8 deficiency in epidermal keratinocytes triggers an inflammatory skin disease. *J Exp Med* 206: 2161–77

Kroncke KD, Fehsel K, Kolb-Bachofen V (1997) Nitric oxide: cytotoxicity versus cytoprotection–how, why, when, and where? *Nitric Oxide* 1:107–20

Li JX, Feng JM, Wang Y *et al.* (2014a) The B-Raf(V600E) inhibitor dabrafenib selectively inhibits RIP3 and alleviates acetaminophen-induced liver injury. *Cell Death Dis* 5:e1278

Li JX, Feng JM, Wang Y *et al.* (2014b) The B-Raf(V600E) inhibitor dabrafenib selectively inhibits RIP3 and alleviates acetaminophen-induced liver injury. *Cell Death Dis* 5:e1278

Man CB, Kwan P, Baum L *et al.* (2007) Association between HLA-B*1502 allele and antiepileptic drug-induced cutaneous reactions in Han Chinese. *Epilepsia* 48:1015–8

Mehta TY, Prajapati LM, Mittal B *et al.* (2009) Association of HLA-B*1502 allele and carbamazepine-induced Stevens-Johnson syndrome among Indians. *Indian J Dermatol Venereol Leprol* 75:579–82

Murata J, Abe R, Shimizu H (2008) Increased soluble Fas ligand levels in patients with Stevens-Johnson syndrome and toxic epidermal necrolysis preceding skin detachment. *J Allergy Clin Immunol* 122:992–1000

Oberst A, Dillon CP, Weinlich R *et al.* (2011) Catalytic activity of the caspase-8-FLIP(L) complex inhibits RIPK3-dependent necrosis. *Nature* 471: 363–7

Palmetshofer A, Zechner D, Luger TA, Barta A (1995) Splicing variants of the human growth hormone mRNA: detection in pituitary, mononuclear cells and dermal fibroblasts. *Mol Cell Endocrinol* 113:225–34

Panayotova-Dimitrova D, Feoktistova M, Ploesser M *et al.* (2013) cFLIP regulates skin homeostasis and protects against TNF-induced keratinocyte apoptosis. *Cell Rep* 5:397–408

Pereira FA, Mudgil AV, Rosmarin DM (2007) Toxic epidermal necrolysis. *J Am Acad Dermatol* 56:181–200

Pierdomenico M, Negroni A, Stronati L *et al.* (2014) Necroptosis is active in children with inflammatory bowel disease and contributes to heighten intestinal inflammation. *Am J Gastroenterol* 109:279–87

Pincelli C, Sevignani C, Manfredini R *et al.* (1994) Expression and function of nerve growth factor and nerve growth factor receptor on cultured keratinocytes. *J Invest Dermatol* 103:13–8

Saito N, Qiao H, Yanagi T *et al.* (2014) An annexin A1-FPR1 interaction contributes to necroptosis of keratinocytes in severe cutaneous adverse drug reactions. *Sci Transl Med* 6:245ra95

Schwartz RA, McDonough PH, Lee BW (2013) Toxic epidermal necrolysis: Part I. Introduction, history, classification, clinical features, systemic manifestations, etiology, and immunopathogenesis. *J Am Acad Dermatol* 69: 173:e1–13

Sun L, Wang H, Wang Z *et al.* (2012) Mixed lineage kinase domain-like protein mediates necrosis signaling downstream of RIP3 kinase. *Cell* 148: 213–27

Vandenabeele P, Galluzzi L, Vanden Berghe T *et al.* (2010) Molecular mechanisms of necroptosis: an ordered cellular explosion. *Nat Rev Mol Cell Biol* 11:700–14

Vanlangenakker N, Vanden Berghe T, Vandenabeele P (2012a) Many stimuli pull the necrotic trigger, an overview. *Cell Death Differ* 19:75–86

Vanlangenakker N, Vanden Berghe T, Vandenabeele P (2012b) Many stimuli pull the necrotic trigger, an overview. *Cell Death Differ* 19:75–86

Ventura JJ, Cogswell P, Flavell RA *et al.* (2004) JNK potentiates TNF-stimulated necrosis by increasing the production of cytotoxic reactive oxygen species. *Genes Dev* 18:2905–15

Viard-Leveugle I, Gaide O, Jankovic D *et al.* (2013) TNF-alpha and IFN-gamma are potential inducers of Fas-mediated keratinocyte apoptosis through activation of inducible nitric oxide synthase in toxic epidermal necrolysis. *J Invest Dermatol* 133:489–98

Wang HY, Sun LM, Su LJ *et al.* (2014) Mixed lineage kinase domain-like protein MLKL causes necrotic membrane disruption upon phosphorylation by RIP3. *Mol Cell* 54:133–46

Wei CY, Chung WH, Huang HW *et al.* (2012) Direct interaction between HLA-B and carbamazepine activates T cells in patients with Stevens-Johnson syndrome. *J Allergy Clin Immunol* 129:1562–9

Wu W, Liu P, Li J (2012) Necroptosis: an emerging form of programmed cell death. *Crit Rev Oncol Hematol* 82:249–58

Wu YT, Tan HL, Huang Q *et al.* (2011) zVAD-induced necroptosis in L929 cells depends on autocrine production of TNFalpha mediated by the PKC-MAPKs-AP-1 pathway. *Cell Death Differ* 18:26–37

Zhang H, Zhou X, McQuade T *et al.* (2011) Functional complementation between FADD and RIP1 in embryos and lymphocytes. *Nature* 471:373–6

Zhao J, Jitkaew S, Cai Z *et al.* (2012) Mixed lineage kinase domain-like is a key receptor interacting protein 3 downstream component of TNF-induced necrosis. *Proc Natl Acad Sci USA* 109:5322–7